UCLA
UCLA Previously Published Works

Title

Excitatory GABAergic Action and Increased Vasopressin Synthesis in Hypothalamic Magnocellular Neurosecretory Cells Underlie the High Plasma Level of Vasopressin in Diabetic Rat.

Permalink

https://escholarship.org/uc/item/7385q549

Journal

Diabetes, 67(3)

ISSN

0012-1797

Authors

Kim, Young-Beom
Kim, Woong Bin
Jung, Won Woo
et al.

Publication Date

2018-03-01

DOI

10.2337/db17-1042

Copyright Information

Peer reviewed

Excitatory GABAergic action and increased vasopressin synthesis in hypothalamic magnocellular neurosecretory cells underlie the high plasma level of vasopressin in diabetic rat.

Young-Beom Kim, Ph.D.[1,2], Woong Bin Kim, Ph.D.[1,2], Won Woo Jung, B.S.[1], Xiangyan Jin, M.D.[1], Yoon Sik Kim[1,3], Byoungjae Kim, Ph.D.[1], Hee Chul Han, M.D., Ph.D.[1,2], Gene D. Block, Ph.D.[3], Christopher S. Colwell, Ph.D.[3] and Yang In Kim, Ph.D.[1,2]

1. Department of Physiology, Korea University College of Medicine, Seoul 136-705,

Republic of Korea

2. Neuroscience Research Institute, Korea University College of Medicine

3. Department of Psychiatry & Biobehavioral Sciences, University of California-Los Angeles,

Los Angeles, CA 90024, U. S. A.

Running title: GABA promotes vasopressin secretion in DM

Y-B Kim and W B Kim contributed equally to this work.

Correspondence: Y. I. Kim, Department of Physiology, Korea University College of Medicine, 126-1 Anam-dong 5-ga, Seoul 136-705, Republic of Korea. E-mail: yikim@korea.ac.kr, phone: 82-2-920-6193 or C. S. Colwell, Department of Psychiatry & Biobehavioral Sciences, University of California-Los Angeles, 760 Westwood Plaza, Los Angeles, CA 90024, U. S. A. E-mail: CColwell@mednet.ucla.edu, phone: 310-909-6887

Total words: 3,995 (main text)

1

Abstract

Diabetes mellitus (DM) is associated with increased plasma levels of arginine-vasopressin (AVP) which may aggravate hyperglycemia and nephropathy. However, the mechanisms by which DM may cause the increased AVP levels are not known. Electrophysiological recordings in the supraoptic nucleus (SON) slices from streptozotocin-induced DM model (STZ) rats and vehicle-treated control rats revealed that GABA functions generally as an excitatory neurotransmitter in the AVP neurons of STZ rats, whereas it evoked usually inhibitory responses in the cells of control animals. Furthermore, Western blot analyses of Cl^- transporters in the SON tissues indicated that NKCC1 (Cl^- importer) was up-regulated and KCC2 (Cl^- extruder) down-regulated in STZ rats. Treatment with CLP290 (KCC2 activator) lowered blood AVP and glucose levels significantly in STZ rats. Lastly, investigation that utilized rats expressing an AVP-enhanced green fluorescent protein fusion gene showed that AVP synthesis in AVP neurons was much more intense in STZ rats than control rats. We conclude that altered Cl^- homeostasis that makes GABA excitatory and enhanced AVP synthesis are important changes in AVP neurons that would increase AVP secretion in DM. Our data suggests that Cl^- transporters in AVP neurons are potential targets of antidiabetic treatment.

Introduction

Diabetes mellitus (DM) is a group of metabolic diseases associated with serious complications such as nephropathy, retinopathy and peripheral neuropathy. Characteristic features of DM include, among others, hyperglycemia and high blood level of arginine-vasopressin (AVP) (1-5). Functional consequences of high AVP level in the blood are unclear. Besides its well-known antidiuretic and vasoconstrictive actions, AVP has been shown to stimulate liver cells to increase their glucose output. AVP has also been shown to increase hepatic glucose output by stimulating the secretion of glucagon from the pancreatic alpha cells (6-8) and ACTH from the anterior pituitary (9,10). In addition, there is some evidence that abundant circulating AVP contributes to increased glomerular filtration, albuminuria and renal hypertrophy in DM (11) through its action at V2 receptors in the kidney (12,13). Furthermore, it has been shown that, in rats with partial nephrectomy, the reduction of AVP secretion induced by increased water intake retards the progression of renal failure (14). Thus, elevated AVP in the blood of DM may contribute to the disease progression (8,15) and directly drive serious diabetic complications, such as renal failure (11).

It is unknown why AVP blood level is markedly elevated in DM, although it is thought that hyperglycemia, in the absence of insulin, greatly increases the hormonal output of AVP neurons by stimulating osmoreceptors (5,16). In this study, we used the streptozotocin (STZ)-induced DM rat model to measure physiological changes in AVP neurons which could underlie the increased hormonal secretion. Here we present evidence that the Cl⁻ importer NKCC1 is up-regulated and the Cl⁻ extruder KCC2 is down-regulated in AVP neurons, thus making GABA excitatory in these cells and that AVP synthesis in magnocellular neurons in the paraventricular (PVN) and supraoptic nuclei (SON) is enhanced. Together these changes would promote the secretion of AVP neurons and, hence, the elevation of AVP blood level

found in DM. Furthermore, we show that the KCC2 activator CLP290 is an effective means

of lowering the blood levels of AVP and glucose in DM, thus raising the possibility that Cl^-

transporter(s) in AVP neurons could be targets of antidiabetic treatment.

Research Design and Methods

Animals. Male Sprague-Dawley rats (6 weeks of age) from Orient Bio (Sungnam, Korea)
and double-transgenic rats of the Wistar strain (6 weeks of age), which express both AVP-
enhanced green fluorescent protein (AVP-eGFP) fusion gene and OXT-monomeric red
fluorescent protein 1 (OXT-mRFP1) fusion gene (17) were used in this study. They were
housed in a 12/12-hour light/dark cycled room for >1 week before being used for
experiments and handled as previously described (18).

DM Model. This model was produced by injecting once the antineoplastic drug STZ to the
rat (65 mg/kg body weight, i.p.). Fresh STZ solutions were prepared before injections by
dissolving the drug (65 mg) in 10 ml of 50-mM sodium citric acid (pH 4.5). Control rats
received the vehicle. Rats were studied 3 weeks after STZ or vehicle injection. To confirm
that STZ injection produced DM, we measured body weight change, blood and CSF glucose
levels (Blood Glucose Meter, Johnson & Johnson, Milpitas, CA), plasma and CSF Na^+
concentrations ($[Na^+]$) (i-Smart 30 VET, i-Sense, Seoul) and osmolalities (Fiske Micro-
Osmometer Model 210, Fiske Associates, Norwood, MA), and plasma AVP level (AVP Elisa
kit; Enzo Life Sciences, Farmingdale, NY).

Hypothalamic slice, electrophysiological recording and Western blot. Eletrophysiological
recordings of SON neurons in hypothalamic slices (350-400-μm thickness) were obtained
extracellularly or intracellularly using gramicidin-perforated technique. Western blot was
performed for the SON tissues excised from hypothalamic slices. The detailed methods for
these experiments were previously described (18,19).

Time of experiments. All experiments were performed during the light or projected light phase.

Drugs. We purchased all drugs and chemicals used in this study from Sigma-Aldrich, except for muscimol (Ascent Scientific, Cambridge, MA). VU0463271, CLP257 and CLP290 were gifts (see Acknowledgments).

Results

STZ treatment is commonly used to produce a DM model. To confirm the

effectiveness of our treatment protocol, we compared the STZ-treated Sprague-Dawley rats

with vehicle-treated ones with respect to various parameters related to DM (**Table I)**. The rats

treated with STZ (STZ rats) gained significantly less body weight than the vehicle-treated

ones (control rats) in the 3-week interval between treatment and experiment. The glucose

concentrations in the blood and CSF and the $[Na^+]$ in the CSF were much higher in the STZ,

than control rats, whereas the plasma $[Na^+]$ was slightly but significantly lower in STZ rats.

Consistent with these observations, the plasma and CSF osmolalities were also significantly

higher in STZ rats. Lastly, the plasma AVP concentrations of STZ rats were ~12 times higher

than those of control animals. Thus, taken together, these results indicate that the STZ

treatment produced DM in Sprague-Dawley rats.

GABA is excitatory in most of the AVP neurons of STZ rats.

AVP neurons in the PVN and SON are heavily innervated by GABAergic afferents

(20), which originate from the perinuclear zones in the hypothalamus (20-22). Through the

$GABA_A$ receptor, GABA exerts an excitatory, rather than inhibitory, effect in most AVP

neurons of chronically salt-loaded, lactating or hypertensive rats (18,19,23,24) in which AVP

secretion is enhanced. Thus, in this study, we examined the possibility that GABA functions

as an excitatory neurotransmitter in the AVP neurons of STZ rats as well, which would

promote the secretory activities of these cells. To test this hypothesis, we first examined the

effects of bath-applied bicuculline ($GABA_A$ receptor antagonist, 30 μM) on the single-unit

activities of the magnocellular neurons recorded extracellularly in the SON slices of control

and STZ rats. In the cells (n=16) of control rats (n=3) bicuculline increased (n=10) or decreased the unit activity (n=6), while in the case of STZ rats (n=3) it decreased the unit activity in all cells (n=16) examined (**Figs. 1A and 1B**). Thus, these results supported the notion that, in general, GABA is excitatory in the AVP neurons of STZ rats whereas it is inhibitory in the cells of control rats. To obtain further evidence for this hypothesis, we next examined $GABA_A$ receptor-mediated postsynaptic potentials (PSPs) recorded in the AVP neurons sampled in the SON slices of control and STZ rats. For the recording of the GABAergic PSPs in isolation from glutamatergic EPSPs, we employed the gramicidin-perforated recording technique, which preserves the intracellular Cl^- concentration ($[Cl^-]_i$) of the recorded cell (25), and included the NMDA receptor blocker DL-2-amino-5-phosphonopentanoic acid (AP-5, 50 μM) and the non-NMDA receptor blocker 6,7-dinitroquinoxaline-2,3-dione (DNQX, 20 μM) in the slice perfusion medium. AVP neurons were identified on the basis of their electrical properties, i.e., little or no inward rectification at membrane potentials between -50 mV and -170 mV (26,27) and/or phasic patterns of firing (28) (**Suppl. Fig. 1**). It was confirmed that the recorded PSPs from AVP neurons were $GABA_A$ receptor-mediated by the inhibitory effects on these synaptic potentials of bicuculline or gabazine (**Suppl. Fig. 2**). **Figs. 1C** and **1D** illustrate that GABAergic PSPs occurring in most of the AVP neurons of STZ rats were excitatory (i.e., EPSPs), whereas those in the cells of control rats were mostly inhibitory (i.e., IPSPs). This difference in GABAergic transmission was apparently due to the difference in the reversal potential of $GABA_A$ receptor-mediated responses (E_{GABA}) (**Fig. 1E & 1F**); in the cells of STZ rats, the E_{GABA} was positive by ~13 mV on average to the action potential threshold, which was around -45 mV, whereas in the cells of control animals, it was negative to the threshold by ~6 mV on average. Collectively, these results indicate that, owing to the depolarizing E_{GABA} shift,

GABA functions as an excitatory, instead of inhibitory, neurotransmitter in most of the AVP

neurons of STZ rats.

To ensure that the observation of GABAergic transmission in the AVP neurons of

STZ-treated Sprague-Dawley rats described above was not strain-specific, that the

identification of AVP neurons based on their electrical properties was valid, and that the

change in GABAergic transmission detected was selective for AVP over oxytocin (OXT)

neurons, we next repeated the gramicidin-perforated recordings of GABAergic transmission

in the AVP and OXT neurons of double-transgenic rats of Wistar strain, which express both

AVP-eGFP fusion gene and OXT-mRFP1 fusion gene. These rats were treated, as were

Sprague-Dawley rats, with STZ or vehicle 3 weeks before SON slice preparation. AVP and

OXT cells in the slice were identified first visually by their green and red fluorescence,

respectively (**Figs. 2A and 2B**), and then, the visual identification was confirmed by the

electrophysiological properties of recorded cell; i.e., for AVP neurons, the presence of phasic

firing and/or little or no inward rectification at membrane potentials between -50 mV and -

170 mV, and for OXT cells, significant inward rectification at membrane potentials between -

50 mV and -170 mV without phasic firing. As in the AVP neurons of Sprague-Dawley rats

treated with STZ, the depolarizing shift of E_{GABA} beyond action potential threshold and the

resultant emergence of GABAergic excitation occurred in most of the AVP neurons of the

STZ-treated transgenic rats (**Figs. 2A and 2C**). Interestingly, however, similar GABAergic

transmission-related events did not occur in the OXT neurons of STZ-treated transgenic rats

(**Figs. 2B and 2D**). Thus, these results indicate that the changes in GABAergic transmission

following STZ treatment occur selectively in AVP neurons and are not strain-dependent.

Furthermore, they indicate that our identification of AVP neurons based on their electrical

properties was valid.

Up-regulation of NKCC1 and down-regulation of KCC2 depolarize E_{GABA} to produce GABAergic excitation in the AVP neurons of STZ rats.

In mammalian central nervous system (CNS) neurons, the Cl^- importer NKCC1 and Cl^- extruder KCC2 play primary roles in regulating $[Cl^-]_i$, the major determinant for E_{GABA} and the polarity of $GABA_A$ receptor–mediated PSP (29). To gain insight into the molecular mechanisms underlying the GABAergic excitation occurring in the AVP neurons of STZ rats, we investigated the expression levels of NKCC1 and KCC2 in the SON using Western blot. The level of NKCC1 was significantly higher and the level of KCC2 was significantly lower in the STZ, than control, rats (**Figs. 3A and 3B**). Thus, these results suggest that, in the diabetic rats, the up-regulation of NKCC1 and the down-regulation of KCC2 in AVP neurons depolarize the E_{GABA} by increasing $[Cl^-]_i$, to cause GABA to function as an excitatory neurotransmitter in these cells. To test this hypothesis more directly, we next examined the effects of the NKCC inhibitor bumetanide (30) and the KCC2 inhibitor VU0463271 (31) on the E_{GABA} and GABAergic PSP profile in the AVP neurons of control and STZ rats. In the neurons (n=13) of control rats (n=5), the bath application of bumetanide (10 μM) did not significantly alter the E_{GABA} (**Fig. 3C, top left**), whereas in the cells (n=16) of STZ rats (n=3), it hyperpolarized the E_{GABA} significantly (**Figure 3C, top right**). The bumetanide effects in these neurons were partially reversible and accompanied by a significant change in the GABAergic PSP profile; i.e., the ratio of neurons showing EPSPs and IPSPs changed from 15:1 to 5:11 after bumetanide application (P<0.001; Fisher exact test). Meanwhile, bath-applied VU0463271 (5 μM) caused a significant depolarization of E_{GABA} in the neurons (n=8) of control rats (n=3; **Fig. 3C, bottom left**) and altered the ratio of neurons showing GABAergic EPSPs and IPSPs from 1:7 to 7:1 (P<0.001; Fisher exact test). In the cells (n=7)

of STZ rats (n=3); however, VU0463271 did not significantly affect the E_{GABA} (**Fig. 3C, bottom right**) and GABAergic PSP profile. Thus, these data, together with the results from the Western blot experiments, indicate that the up-regulation of NKCC1 and the down-regulation of KCC2 are the molecular mechanisms which underlie the depolarizing shift of E_{GABA} and the consequent emergence of GABAergic excitation in the AVP neurons of STZ rats.

AVP synthesis is enhanced in the AVP neurons of STZ rats.

The results described above demonstrate that GABAergic inhibition is converted into excitation in the AVP neurons of STZ rats, thus indicating that the process of AVP release is enhanced in these cells. To maintain increased hormone secretion in a given neuron, the synthesis of the hormone, as well as its release process, should be enhanced. To see if AVP synthesis was enhanced in the AVP neurons of STZ rats, we compared the STZ-treated Wistar rats expressing both AVP-eGFP and OXT-mRFP1 fusion genes with the vehicle-treated control animals with respect to the intensities of green and red fluorescence in the SON and the magnocellular division of the PVN. As expected, the green fluorescence intensity was significantly higher in both hypothalamic regions of the STZ rats than the control rats (**Figs. 4A and 4B**). On the other hand, red fluorescence intensity was not different between the two rat groups in both the SON and PVN (**Figs. 4A and 4C**). Thus, these results indicate that the synthesis of AVP, but not OXT, is enhanced in hypothalamic magnocellular neurosecretory cells of the STZ rats.

Systemic administration of the KCC2 activator CLP290 in the STZ rat lowers AVP and glucose levels in the blood.

The results presented above indicate that the inhibitory-to-excitatory switch in

GABAergic transmission in the AVP neurons of STZ rats, an electrophysiological change that

would promote the release of AVP from these cells, arises from the up-regulation of NKCC1

and the down-regulation of KCC2. Thus, we reasoned that the blockade of NKCC1 or the

activation of KCC2 might decrease AVP release by preventing the GABAergic excitation of

AVP neurons. Moreover, we thought that they might lower the blood glucose level as well

since AVP increases the blood sugar by stimulating hepatic gluconeogenesis and

glycogenolysis (6-8). To see if KCC2 activation in STZ rats can lower the AVP and glucose

levels in the blood, we examined the effects on these variables of CLP290, a prodrug of the

KCC2 activator CLP257 (32). Before we test the effects of CLP290 on the AVP and glucose

levels in the blood, we first investigated whether KCC2 activation with CLP257 prevented

the GABAergic excitation, by assessing the effects of this agent on the E_{GABA} and

GABAergic PSP profile in the AVP neurons recorded in the SON slices of STZ rats. The

effects of CLP257 were evaluated by comparing the electrophysiological data from SON

slices incubated for 2 h in this agent (25 μM) with those from slices kept in the vehicle

DMSO (0.025%) for the same duration. The AVP neurons sampled in the slices treated with

CLP257 had more hyperpolarized E_{GABA} (**Fig. 5A**) and significantly lower ratio of

GABAergic EPSPs vs. IPSPs than the ones recorded in vehicle-treated slices (3:6 vs. 9:1;

P=0.02; Fisher exact test). On the other hand, the AVP neurons sampled in the SON slices

from control rats treated with CLP257 were not different from the cells in the vehicle-treated

slices from the same rat group in E_{GABA} (**Fig. 5A**) and GABAergic PSP profile (ratio of

GABAergic EPSPs vs. IPSPs; 1:8 to 0:11). Therefore, these results indicate that the KCC2

activation with CLP257 prevents GABAergic excitation in the AVP neurons of STZ rats.

Therefore, we continued to examine the effects of CLP290 on AVP and glucose levels in the

blood. CLP290 (100 mg/kg body weight) or vehicle (20% HPCD) was injected intraperitoneally 4 h prior to the blood sampling for the measurements of AVP and glucose concentrations. As illustrated in **Figures 5B** and **5C**, CLP290 treatment in STZ rats significantly lowered AVP and glucose levels, while in control rats it resulted in a significant increase in the plasma AVP level without affecting the glucose concentration.

Discussion

The elevated blood level of AVP in DM can aggravate hyperglycemia (6-9) and contribute to the generation of diabetic nephropathy (11). Despite such potential significance of high blood level of AVP, the mechanisms underlying the elevation of AVP level have not been fully identified. In the current study, we focused on the possible changes occurring in the AVP neurons that would promote their hormone secretion under disease conditions. Secretion of a neurohormone or neurotransmitter from a neuron involves two processes: the synthesis and release of secreted substance. In mature CNS neurons, the release process is governed by the action potential firing, which is in turn regulated mainly by the balance of excitatory glutamatergic and inhibitory GABAergic transmission. Given that AVP neurons are densely innervated by GABAergic afferents (20) and that GABA functions as excitatory, instead of inhibitory, neurotransmitter in the majority of AVP neurons of chronically salt-loaded, lactating or hypertensive rats (18,19,23,24) in which AVP secretion is enhanced, we scrutinized GABAergic transmission in the current study. We found that the E_{GABA} depolarized significantly, and therefore, GABA became excitatory in the majority of AVP neurons of our DM model rats. On the other hand, GABA was mostly inhibitory in the cells of normal (i.e., control) rats, as previously reported (19, 23). Furthermore, we discovered that the synthesis of AVP is greatly increased in the SON and the magnocellular region of the PVN of DM model rats. Thus, our results suggest that increased secretory activities of AVP neurons, due to the enhancement of AVP synthesis and the modulation of GABAergic transmission, contribute to the escalation of blood level of AVP in DM.

AVP neurons are heavily innervated not only by GABAergic inputs, but also by glutamatergic afferents originating from various brain regions including the organum vasculosum of the lamina terminalis, the subfornical organ and the median preoptic nucleus

14

(33). In a previous study, Di and Tasker (34) showed that dehydration induced by chronic salt

loading, which leads to enhanced AVP secretion, increased EPSC amplitude and frequency in

magnocellular neurons of the rat SON. Thus, the increased secretory activities of AVP

neurons in DM may depend on the modulation of glutamatergic (as well as GABAergic)

transmission. The determination of the importance of glutamatergic transmission for the

enhancement of AVP secretion in the present model awaits future studies.

In the current study, we discovered that STZ treatment resulted in the depolarizing

shift of E_{GABA} and consequent emergence of GABAergic excitation in AVP but not OXT

neurons. This finding contrasts with the observations made in our previous study performed

with rats in which E_{GABA} depolarized and GABAergic excitation emerged in both AVP and

OXT neurons after chronic salt loading (19). The absence of such changes in the OXT

neurons of DM model rats makes sense because the emergence of GABAergic excitation in

this neuronal population would enhance the secretion of OXT, a hormone which is known to

stimulate the secretion of atrial natriuretic hormone from the atrium (35) and act directly in

the kidney to promote natriuresis (36,37). The enhanced secretion of OXT would aggravate

the hyponatremia present in these animals.

The strength and polarity of synaptic responses mediated by $GABA_A$ receptor are

determined primarily by $[Cl^-]_i$. The results obtained from our Western blot and

neurophysiological experiments indicate that the depolarizing shift of E_{GABA} and the resultant

emergence of GABAergic excitation detected in the AVP neurons of DM model rats,

electrophysiological changes which would promote the secretory activities of these cells,

were due to the increase in $[Cl^-]_i$ that resulted from the up-regulation of the Cl^- importer

NKCC1 and down-regulation of the Cl^- extruder KCC2. This conclusion is corroborated by

the finding that the systemic administration of the KCC2 activator CLP290 resulted in a

15

significant reduction of the blood level of AVP in the DM model rat. In the present study, we did not investigate the possible mechanisms that would lead to the changes in NKCC1 and KCC2 expression. The mechanism that causes NKCC1 up-regulation may involve the activation of autoreceptors by AVP, a paracrine released from the somata and dendrites of AVP neurons in response to hyperglycemia and perhaps to the increase in osmolality and [Na^+] of the CSF. In accordance with this idea, Ludwig (38) has demonstrated that hyperosmotic stress is a good stimulus for AVP release from the somata and dendrites of hypothalamic magnocellular neurons in the rat. Additionally, we have shown that, in rats subjected to chronic hyperosmotic stress, the cerebroventricular administration of the V1a AVP receptor antagonist $d(CH_2)_5[Tyr(Me)^2, Ala-NH_2^9]AVP$ significantly lowers the proportion of magnocellular neurons in the SON that exhibit GABAergic excitation, a phenomenon resulting from the up-regulation of NKCC1 (19). Furthermore, Wakamatsu and colleagues (39) showed that AVP increases the expression of NKCC1 in the outer medullary collecting duct of the rat nephron.

Meanwhile, the mechanism underlying the KCC2 down-regulation in the AVP neurons of DM model rats may involve the action of BDNF, which is released locally from glia and/or neurons in the PVN and SON. It has been shown that hyperosmotic stimulus increases the local release of BDNF in the SON (40) and that the BDNF receptor tropomyosin-receptor-kinase B (TrkB) is present in the SON (23,40,41). Furthermore, it has been reported that chronic salt loading in the rat prevents the GABAergic inhibition of AVP neurons by KCC2 down-regulation via the BDNF-dependent activation of TrkB (23). In the present study, we demonstrated that CLP257, a drug that activates KCC2 by apparently inhibiting BDNF action (32), hyperpolarized E_{GABA} and hence converted GABAergic excitation back to inhibition in the AVP neurons of DM model rats. Lastly, it has been shown

that, in a rat model of neuropathy produced by applying polyethylene cuffs to the sciatic nerve, BDNF from microglia downregulates KCC2 expression through TrkB, enabling GABAergic excitation to occur in neurons in the lamina I of the spinal dorsal horn. This paradoxical excitation contributes to the generation of neuropathic pain in this animal model (42). More recently, however, Morgado and colleagues (43) reported that, in STZ-induced diabetic rats, BDNF level is not altered in the spinal cord and neuropathic pain is not much affected by the BDNF sequester TrkB/Fc, despite the fact that spinal KCC2 down-regulation, which causes the inhibitory-to-excitatory switch of GABAergic action to occur, underlies the generation of neuropathic pain (44,45). Thus, they suggested that BDNF-induced KCC2 down-regulation is less likely to be responsible for the generation of GABAergic excitation in the spinal neurons and neuropathic pain in this animal model. Further investigation is required to determine if the mechanisms underlying the changes in NKCC1 and KCC2 expression in the AVP neurons of our DM model rats involve the AVP activation of autoreceptor and the BDNF activation of TrkB.

In this study, we found that the intraperitoneal injection of the KCC2 activator CLP290 in STZ-induced DM rats lowered the blood level of AVP by ~50% and glucose by ~15%. These results not only support the notion that the down-regulation of KCC2 is partly responsible for the depolarizing shift of E_{GABA} and the emergence of GABAergic excitation in the AVP neurons of DM model rats (see above), but they also suggest that this drug is an effective means of lowering the blood level of AVP and glucose in DM. The smaller effect of CLP290 on the blood sugar than AVP level may be related to the fact that the effects of AVP on glycogenolysis and gluconeogenesis (7,8) in the liver are reduced in DM due to the down-regulation of hepatic V1a receptors (46,47) and to the fact that AVP is not the only factor contributing to the escalation of the blood sugar in DM.

The increase in the plasma AVP level of control rats after CLP290 treatment was an unexpected finding, raising the possibility that non-specific effects on cells other than AVP neurons are involved in CLP290 administration *in vivo*. However, it seems unlikely that the rise of AVP level resulted from GABAergic excitation in AVP neurons in the light of the observation that the KCC2 activator CLP257 did not depolarize the E_{GABA} in these cells. Also, it is unlikely that the plasma AVP concentration was increased by osmotic stimulation because the intraperitoneally injected drug solution was rather hypoosmotic (~270 mOsm/Kg H_2O).

In summary, we provide evidence that altered Cl^- homeostasis in AVP neurons and the enhanced AVP synthesis in these cells are important changes underlying the increase in the plasma AVP level in DM. With growing evidence that elevated AVP in the DM blood is a risk factor for metabolic disorders (8,15) and progression of serious diabetic complications like nephropathy (11), future studies evaluating the possible effects of drugs including CLP290 that target Cl^- transporters against diabetic complications are warranted.

Acknowledgements

Author Contributions

Y.-B.K., W.B.K, H.C.H., G.D.B, C.S.C. and Y.I.K, conceived this project. Y.-B.K., W.B.K., W.W.J, X.J, Y.S.K. and B.J.K. performed the experiments and analyzed the results. Y.-B.K., W.B.K, C.S.C. and Y.I.K. wrote the manuscript.

References

1.   Zerbe RL, Vinicor F, Robertson GL. Plasma vasopressin in uncontrolled diabetes mellitus. *Diabetes* 1979; 28:503-508.

2.   Iwasaki Y, Kondo K, Murase T, Hasegawa H, Oiso Y. Osmoregulation of plasma vasopressin in diabetes mellitus with sustained hyperglycemia. *Journal of neuroendocrinology* 1996; 8:755-760.

3.   Kamoi K, Ishibashi M, Yamaji T. Thirst and plasma levels of vasopressin, angiotensin II and atrial natriuretic peptide in patients with non-insulin-dependent diabetes mellitus. *Diabetes research and clinical practice* 1991; 11:195-202.

4.   Van Itallie CM, Fernstrom JD. Osmolal effects on vasopressin secretion in the streptozotocin-diabetic rat. *The American journal of physiology* 1982; 242:E411-417.

5.   Brooks DP, Nutting DF, Crofton JT, Share L. Vasopressin in rats with genetic and streptozocin-induced diabetes. *Diabetes* 1989; 38:54-57.

6.   Hems DA, Whitton PD. Stimulation by vasopressin of glycogen breakdown and gluconeogenesis in the perfused rat liver. *The Biochemical journal* 1973; 136:705-709.

7.   Kirk CJ, Hems DA. Hepatic action of vasopressin: lack of a role for adenosine-3',5'-cyclic monophosphate. *FEBS letters* 1974; 47:128-131.

8.   Yibchok-anun S, Abu-Basha EA, Yao CY, Panichkriangkrai W, Hsu WH. The role of arginine vasopressin in diabetes-associated increase in glucagon secretion. *Regulatory peptides* 2004; 122:157-162.

9.   Yates FE, Maran JW. The physiology of the mammalian hypothalamo-adenopophysal-adrenal glucocorticoid system - a new hypothesis. *Chronobiologia* 1974; 1 Suppl 1:195-223.

10.   Krieger DT, and E. A. Zimmerman. The nature of CRF and its relationship to vasopressin. New York: Academic Press, INC.; 1977.

11.   Bardoux P, Martin H, Ahloulay M*, et al.* Vasopressin contributes to hyperfiltration, albuminuria, and renal hypertrophy in diabetes mellitus: study in vasopressin-deficient Brattleboro rats. *Proceedings of the National Academy of Sciences of the United States of America* 1999; 96:10397-10402.

12.   Bankir L, Bardoux P, Ahloulay M. Vasopressin and diabetes mellitus. *Nephron* 2001; 87:8-18.

13.   Bardoux P, Bruneval P, Heudes D, Bouby N, Bankir L. Diabetes-induced albuminuria: role of antidiuretic hormone as revealed by chronic V2 receptor antagonism in rats. *Nephrology, dialysis, transplantation : official publication of the European Dialysis and Transplant Association - European Renal Association* 2003; 18:1755-1763.

14.   Bouby N, Bachmann S, Bichet D, Bankir L. Effect of water intake on the progression of chronic renal failure in the 5/6 nephrectomized rat. *The American journal of physiology* 1990; 258:F973-979.

15.   Bodnar RJ, Wallace MM, Kordower JH*, et al.* Modulation of nociceptive thresholds by vasopressin in the Brattleboro and normal rat. *Annals of the New York Academy of Sciences* 1982; 394:735-739.

16.   Vokes TP, Aycinena PR, Robertson GL. Effect of insulin on osmoregulation of vasopressin. *The American journal of physiology* 1987; 252:E538-548.

17.   Katoh A, Fujihara H, Ohbuchi T*, et al.* Highly visible expression of an oxytocin-monomeric red fluorescent protein 1 fusion gene in the hypothalamus and posterior pituitary of transgenic rats. *Endocrinology* 2011; 152:2768-2774.

18.   Kim YB, Kim YS, Kim WB*, et al.* GABAergic excitation of vasopressin neurons:

possible mechanism underlying sodium-dependent hypertension. *Circulation research* 2013; 113:1296-1307.

19. Kim JS, Kim WB, Kim YB*, et al.* Chronic hyperosmotic stress converts GABAergic inhibition into excitation in vasopressin and oxytocin neurons in the rat. *The Journal of neuroscience : the official journal of the Society for Neuroscience* 2011; 31:13312-13322.

20. Decavel C, Van den Pol AN. GABA: a dominant neurotransmitter in the hypothalamus. *The Journal of comparative neurology* 1990; 302:1019-1037.

21. Boudaba C, Szabo K, Tasker JG. Physiological mapping of local inhibitory inputs to the hypothalamic paraventricular nucleus. *The Journal of neuroscience : the official journal of the Society for Neuroscience* 1996; 16:7151-7160.

22. Theodosis DT, Paut L, Tappaz ML. Immunocytochemical analysis of the GABAergic innervation of oxytocin- and vasopressin-secreting neurons in the rat supraoptic nucleus. *Neuroscience* 1986; 19:207-222.

23. Choe KY, Han SY, Gaub P*, et al.* High salt intake increases blood pressure via BDNF-mediated downregulation of KCC2 and impaired baroreflex inhibition of vasopressin neurons. *Neuron* 2015; 85:549-560.

24. Lee SW, Kim YB, Kim JS*, et al.* GABAergic inhibition is weakened or converted into excitation in the oxytocin and vasopressin neurons of the lactating rat. *Molecular brain* 2015; 8:34.

25. Rhee JS, Ebihara S, Akaike N. Gramicidin perforated patch-clamp technique reveals glycine-gated outward chloride current in dissociated nucleus solitarii neurons of the rat. *Journal of neurophysiology* 1994; 72:1103-1108.

26. Hirasawa M, Mouginot D, Kozoriz MG, Kombian SB, Pittman QJ. Vasopressin differentially modulates non-NMDA receptors in vasopressin and oxytocin neurons in the

supraoptic nucleus. *The Journal of neuroscience : the official journal of the Society for Neuroscience* 2003; 23:4270-4277.

27.   Stern JE, Armstrong WE. Electrophysiological differences between oxytocin and vasopressin neurones recorded from female rats in vitro. *The Journal of physiology* 1995; 488 (Pt 3):701-708.

28.   Yamashita H, Inenaga K, Kawata M, Sano Y. Phasically firing neurons in the supraoptic nucleus of the rat hypothalamus: immunocytochemical and electrophysiological studies. *Neuroscience letters* 1983; 37:87-92.

29.   Ben-Ari Y. Excitatory actions of gaba during development: the nature of the nurture. *Nature reviews Neuroscience* 2002; 3:728-739.

30.   Payne JA, Rivera C, Voipio J, Kaila K. Cation-chloride co-transporters in neuronal communication, development and trauma. *Trends in neurosciences* 2003; 26:199-206.

31.   Delpire E, Baranczak A, Waterson AG*, et al.* Further optimization of the K-Cl cotransporter KCC2 antagonist ML077: development of a highly selective and more potent in vitro probe. *Bioorganic & medicinal chemistry letters* 2012; 22:4532-4535.

32.   Gagnon M, Bergeron MJ, Lavertu G*, et al.* Chloride extrusion enhancers as novel therapeutics for neurological diseases. *Nature medicine* 2013; 19:1524-1528.

33.   Csaki A, Kocsis K, Kiss J, Halasz B. Localization of putative glutamatergic/aspartatergic neurons projecting to the supraoptic nucleus area of the rat hypothalamus. *The European journal of neuroscience* 2002; 16:55-68.

34.   Di S, Tasker JG. Dehydration-induced synaptic plasticity in magnocellular neurons of the hypothalamic supraoptic nucleus. *Endocrinology* 2004; 145:5141-5149.

35.   Haanwinckel MA, Elias LK, Favaretto AL*, et al.* Oxytocin mediates atrial natriuretic peptide release and natriuresis after volume expansion in the rat. *Proceedings of the National*

Academy of Sciences of the United States of America 1995; 92:7902-7906.

36. Balment RJ, Brimble MJ, Forsling ML. Release of oxytocin induced by salt loading and its influence on renal excretion in the male rat. *The Journal of physiology* 1980; 308:439-449.

37. Verbalis JG, Mangione MP, Stricker EM. Oxytocin produces natriuresis in rats at physiological plasma concentrations. *Endocrinology* 1991; 128:1317-1322.

38. Ludwig M. Dendritic release of vasopressin and oxytocin. *Journal of neuroendocrinology* 1998; 10:881-895.

39. Wakamatsu S, Nonoguchi H, Ikebe M*, et al.* Vasopressin and hyperosmolality regulate NKCC1 expression in rat OMCD. *Hypertension research : official journal of the Japanese Society of Hypertension* 2009; 32:481-487.

40. Arancibia S, Lecomte A, Silhol M, Aliaga E, Tapia-Arancibia L. In vivo brain-derived neurotrophic factor release and tyrosine kinase B receptor expression in the supraoptic nucleus after osmotic stress stimulus in rats. *Neuroscience* 2007; 146:864-873.

41. Marmigere F, Rage F, Tapia-Arancibia L, Arancibia S. Expression of mRNAs encoding BDNF and its receptor in adult rat hypothalamus. *Neuroreport* 1998; 9:1159-1163.

42. Coull JA, Beggs S, Boudreau D*, et al.* BDNF from microglia causes the shift in neuronal anion gradient underlying neuropathic pain. *Nature* 2005; 438:1017-1021.

43. Morgado C, Pereira-Terra P, Cruz CD, Tavares I. Minocycline completely reverses mechanical hyperalgesia in diabetic rats through microglia-induced changes in the expression of the potassium chloride co-transporter 2 (KCC2) at the spinal cord. *Diabetes, obesity & metabolism* 2011; 13:150-159.

44. Jolivalt CG, Lee CA, Ramos KM, Calcutt NA. Allodynia and hyperalgesia in diabetic rats are mediated by GABA and depletion of spinal potassium-chloride co-

transporters. *Pain* 2008; 140:48-57.

45.   Morgado C, Pinto-Ribeiro F, Tavares I. Diabetes affects the expression of GABA and potassium chloride cotransporter in the spinal cord: a study in streptozotocin diabetic rats. *Neuroscience letters* 2008; 438:102-106.

46.   Trinder D, Phillips PA, Stephenson JM*, et al.* Vasopressin V1 and V2 receptors in diabetes mellitus. *The American journal of physiology* 1994; 266:E217-223.

47.   Phillips PA, Risvanis J, Hutchins AM*, et al.* Down-regulation of vasopressin V1a receptor mRNA in diabetes mellitus in the rat. *Clinical science* 1995; 88:671-674.

48.   Murase K, Ryu PD, Randic M. Excitatory and inhibitory amino acids and peptide-induced responses in acutely isolated rat spinal dorsal horn neurons. *Neuroscience letters* 1989; 103:56-63.

Table 1

Contents	Control	*n*	STZ	*n*
△ Body weight (g)	138.6 ± 26.6	15	38.9 ± 39.5 **	15
Blood glucose levels (mg/dl)	143.1 ± 42.4	15	512.7 ± 89.2 **	15
CSF glucose levels (mg/dl)	103.7 ± 11.1	15	264.6 ± 68.8 **	15
Plasma [Na^+] (mmol/L)	137.1 ± 2.5	15	132.2 ± 4.5**	15
CSF [Na^+] (mmol/L)	148.2 ± 1.2	15	154.3 ± 5.4**	15
Plasma osmolality (mOsm/KgH_2O)	322.3 ± 5.3	15	344.5 ± 13.3 **	15
CSF osmolality (mOsm/KgH_2O)	324.5 ± 4.5	15	340.7 ± 10.9 **	15
Plasma AVP levels (pg/ml)	5.8 ± 5.6	9	68.6 ± 72.1 *	12

* $P < 0.05$, ** $P < 0.001$, student's *t*-test or Rank Sum test

(Values are shown as mean ± SD)

Table I: Data showing body weight changes and the [glucose], [Na^+], osmolality and [AVP] of the blood, plasma or CSF in the control and STZ model rats. n: number of rats. Blood samples for glucose level and [Na^+] measurements were obtained from the tail vein without anesthesia, while the blood samples for plasma osmolality and AVP level measurements were obtained by decapitation under urethane anesthesia (1.25 g/kg body weight, i.p.). In order to prevent clotting and protease action, these samples were collected in 3-ml BD vacutainer containing K_2-EDTA (Franklin Lakes, NJ) and aprotinin (0.6 TIU/ml blood). The plasma was obtained by centrifuging the blood at 1,600 x g for 15 min at 4º C and used immediately for osmolality measurement or stored in a deep freezer (-80º C) until used for AVP Elisa. CSF samples were obtained through the atlanto-occipital membrane just before the blood sampling by decapitation.

Figure legends

Figure 1: GABA$_A$ receptor-mediated transmission in the AVP neurons of control and STZ model rats. (A) Extracellular single-unit recordings in magnocellular neurons sampled in the SON slices from control and STZ rats, which show the effects of bicuculline (30 μM, bath-applied) on spontaneous firing. The single-unit recordings were performed after raising the baseline firing with the use of 20-mM KCl-containing slice perfusion medium, because most AVP neurons were silent in the *in-vitro* slice condition. (B) Graphs summarizing the reversible effects of bicuculline on spontaneous firing in the magnocellular neurons of control and STZ groups. The bar charts denote means ± SD's. Sixteen cells each were recorded from the control and STZ rat groups, and for each rat, 4-6 cells were sampled. (C-F) Data from gramicidin-perforated patch recording technique. (C) Voltage traces showing spontaneously occurring GABA$_A$ receptor-mediated IPSPs (○) and EPSPs (●) recorded after the blockade

of glutamatergic transmission with the use of the cocktail of the NMDA receptor blocker DL-2-amino-5-phosphonopentanoic acid (AP-5, 50 μM) and the non-NMDA receptor blocker 6,7-dinitroquinoxaline-2,3-dione (DNQX, 20 μM). The arrows denote action potentials arising from EPSPs. The baseline membrane potential is indicated to the left of each voltage trace. (D) Proportions of cells exhibiting GABA$_A$ receptor-mediated IPSPs and EPSPs. n: number of cells examined (SON slices from 15 rats were used for each rat group). (E) Estimation of E$_{GABA}$. Insets: Whole-cell currents elicited by the GABA$_A$ receptor agonist muscimol (▲ 10 μM; 10 ms) applied focally (48) at various holding potentials (V$_H$) in the presence of AP-5 (50 μM) and DNQX (20 μM). The muscimol-elicited currents measured at the peaks are plotted against V$_H$, and linear regression was used to fit these data points. The

intersection of regression line with the abscissa denoted with arrow was taken as the reversal

potential of the muscimol-elicited currents (i.e., E_{GABA}). (F) Box plots of the E_{GABA} values

estimated for the AVP neurons of control and STZ groups. n: number of cells examined (SON

slices from 15 rats were used for each rat group). **: P<0.001 compared with the value

before drug treatment (One-way repeated measures ANOVA followed by pairwise

comparison with Holm-Sidak procedure) (B). **: P<0.001 (Fisher exact test) (D). **:

P<0.001 (Student's *t*-test) (F).

Figure 2: Depolarizing shift of E_{GABA} and the resultant emergence of GABAergic excitation

occur in the AVP, but not OXT, neurons of STZ model rats. (A & B) Visualization of AVP and

OXT neurons in the SON slices prepared from double-transgenic rats expressing both the

AVP-enhanced green fluorescent protein (AVP-eGFP) fusion gene and OXT-monomeric red

fluorescent protein 1 (OXT-mRFP1) fusion gene. Left and right panels: images of the same

fields taken under bright field and epifluorescence illumination, respectively. Asterisks denote

recorded cells. (C & D) Mean (±SD) E_{GABA} values estimated for and the proportions of cells

exhibiting $GABA_A$ receptor-mediated IPSPs and EPSPs in the AVP (C) and OXT (D) neurons

of control and STZ rats. SON slices from 7 control and 6 STZ rats were used for these

electrophysiological recordings. n: number of cells examined. **: P<0.001, NS: not

significant (C & D, left panels, Student's *t*-test or Rank Sum test; C & D, right panels, Fisher

exact test).

Figure 3: Up-regulation of Na^+-K^+-$2Cl^-$ cotransporter isotype 1 (NKCC1) and down-

regulation of K^+-Cl^- cotransporter isotype 2 (KCC2) expression in the AVP neurons of STZ

model rats. (A) NKCC1, KCC2, and β-actin bands recognized by Western blot for the SON

28

tissue samples obtained from control and STZ model rats. (B) Bar graphs showing the relative levels of NKCC1 and KCC2 in the SON of control and model rats. For each experiment, the values were normalized to the average value of the samples collected from control rats. Since the SON is a small structure, SON tissues from 3 rats were pooled to form a single sample. NKCC1 and KCC2 levels were normalized to β-actin to control for loading. n: number of experiments repeated. (C) Graphs illustrating the effects of KCC2 blocker VU0463271 (5 μM) and NKCC1 inhibitor bumetanide (10 μM) on E_{GABA} in AVP neurons recorded in the SON slices from control and model rats. Bumetanide solution was prepared by diluting its 0.1-M NaOH-based stock solution with ACSF, while VU0463271 by diluting its dimethylsulfoxide (DMSO)-based stock solution with ACSF. The symbols connected by lines denote data from the same cells. Data from 3-5 rats. Values in (B) and (C) are shown as mean ± SD. *: P<0.05 (Student's *t*-test) (B). NS: not significant, *: P<0.05 and **: P<0.001 compared with the value before drug treatment (One-way repeated measures ANOVA followed by pairwise comparison with Holm-Sidak procedure) (C).

Figure 4: AVP, but not OXT, synthesis was enhanced in the SON and the magnocellular region of the PVN. (A) Representative photomicrographs illustrating the expression of AVP-eGFP and OXT-mRFP1 in the SON and PVN of control and STZ model rats. (B & C) Graphs showing the mean (± SD) fluorescence intensities for AVP-eGFP and OXT-mRFP in the SON and the magnocellular division of the PVN. NS: not significant, **: P<0.001 (One-way ANOVA followed by pairwise comparison with Holm-Sidak procedure). n: number of rats. Paraformaldehyde (4%)-fixed hypothalamic sections (30-μm thickness) mounted on the slide glass in the mounting medium with DAPI (Vector Laboratories, Burlingame, CA) were examined for the fluorescence intensities of eGFP and mRFP1 in the SON and the

magnocellular region of the PVN, with the use of a confocal fluorescent microscope (Carl Zeiss LSM 700) and the *imageJ* software. For standardization in quantifying eGFP/mRFP1 fluorescence across slices and animals, we tried to compare similar portions of the SON and PVN and used rats with the same age. Also, animals used for this analysis were killed at the same time of the day (i.e., at zeitgeber time 2 hour, with 0 hour being lights on in the animal room), given the diurnal nature of AVP expression.

Fig. 5: Effects of the KCC2 activators CLP257 and CLP290 on the E_{GABA} of AVP neurons and the plasma AVP and blood glucose levels in the control and STZ rats. (A) CLP257: 25 µM. CLP257 solution was prepared by diluting its DMSO-based stock solutions with ACSF. n: number of cells recorded (data for each experimental group were obtained from 3-4 rats). (B & C) CLP290: 100 mg/kg body weight. CLP290 solution for intraperitoneal injection was made by dissolving 100 mg of CLP290 in 10 ml of 20% hydroxypropyl-β-cyclodextrin (HPCD). n: number of rats. Values in (A-C) are shown as mean ± SD. NS: not significant. *: P<0.05, **: P<0.001 (Student's *t*-test or Rank Sum test).
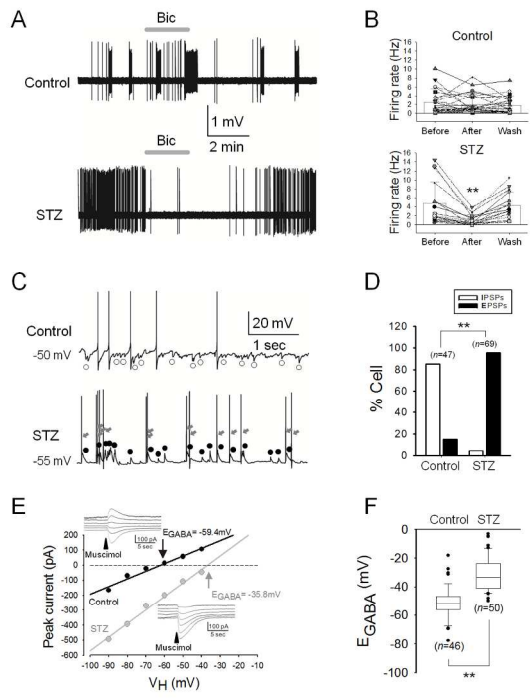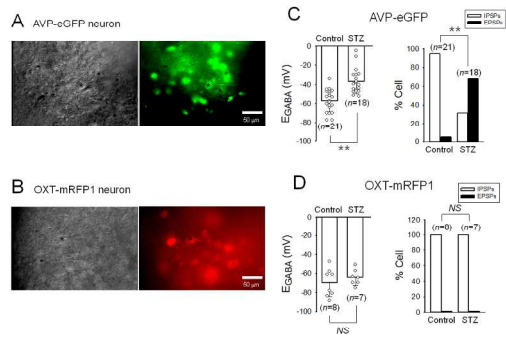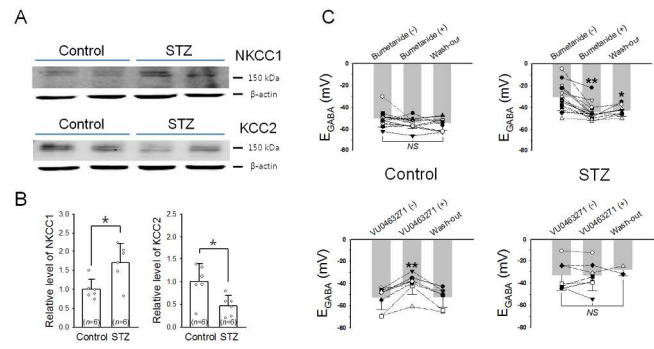
Fig. 1

Fig. 1

593x419mm (96 x 96 DPI)

Fig. 2

A   AVP-eGFP neuron

B   OXT-mRFP1 neuron

C   AVP-eGFP

D   OXT-mRFP1

593x419mm (96 x 96 DPI)

Fig. 3

593x419mm (96 x 96 DPI)
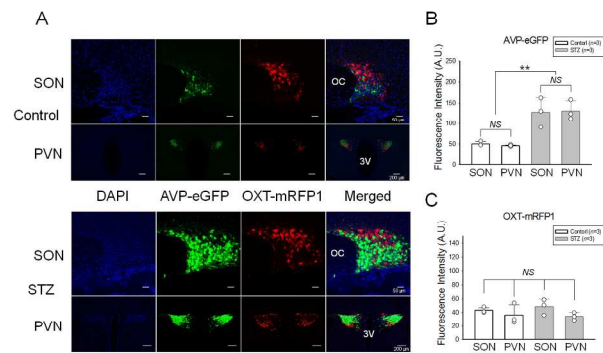
Fig. 4

Fig. 4

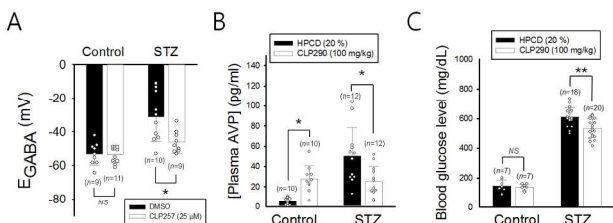593x419mm (96 x 96 DPI)

Fig. 5

Fig. 5

593x419mm (96 x 96 DPI)

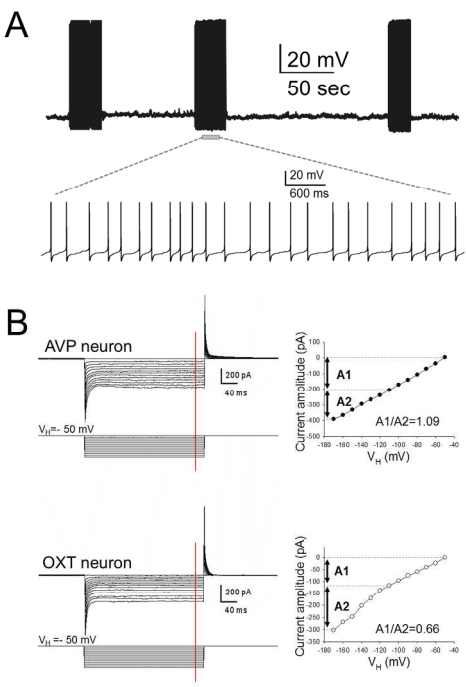**<Supplemental Materials>**

Supplemental figure legends

Suppl. Fig. 1: Identification of AVP-expressing neurons. (A) *Top panel*: Voltage trace showing phasic firing pattern that characterizes AVP neurons. *Bottom panel*: Time-expanded trace of the portion indicated in the top panel. (B) *Left panel*: current responses evoked by a series of hyperpolarizing voltage pulses (300-ms duration) applied at the holding potential (V_H) of -50 mV with 10-mV increments in putative AVP and OXT neurons. The voltage protocol is shown below the current traces. The red vertical line in each set of traces denotes the time point at which current amplitude was measured. *Right panel*: Plots showing the current-voltage relations of putative AVP and OXY neurons. The ratio of current amplitude denoted with A1 (i.e., difference current between V_H of -50 mV and -110 mV) and A2 (i.e., difference current between V_H of -110 mV and -170 mV) was taken as a criterion for classifying the recorded cell as putative AVP or OXY neuron. A1/A2 >0.8 indicated putative AVP neuron, while one ≤0.8 OXY neuron.

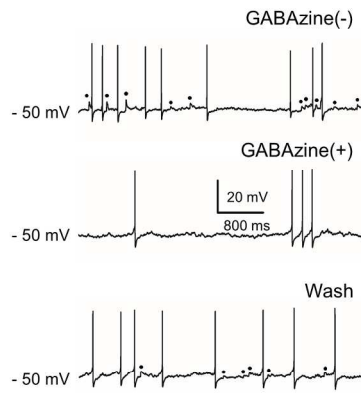Suppl. Fig. 2: Inhibitory effect of the $GABA_A$ receptor antagonist gabazine on spontaneous GABAergic EPSPs recorded in an AVP neuron sampled in the SON slice from STZ rat. Gabazine (5 μM) was bath-applied to the slice. The GABAergic EPSPs (●) were isolated from glutamatergic EPSPs by including in the slice perfusion medium the NMDA receptor antagonist AP-5 (50 μM) and the non-NMDA receptor antagonist DNQX (20 μM). The inhibitory effect of gabazine on the GABAergic EPSPs reversed about 10 min after the washout of the drug.

Suppl. 1

593x420mm (96 x 96 DPI)

Suppl. 2

GABAzine(-)

- 50 mV

GABAzine(+)

20 mV

800 ms

- 50 mV

Wash

- 50 mV

593x420mm (96 x 96 DPI)